Electric field driven magnetic phase transition in graphene nanoflakes

Aiping Zhou, Weidong Sheng, and S. J. Xu

Citation: Applied Physics Letters **103**, 133103 (2013); doi: 10.1063/1.4821954
View online: http://dx.doi.org/10.1063/1.4821954
View Table of Contents: http://scitation.aip.org/content/aip/journal/apl/103/13?ver=pdfcov
Published by the AIP Publishing

Electric field driven magnetic phase transition in graphene nanoflakes

Aiping Zhou,[1] Weidong Sheng,[2,a)] and S. J. Xu[3]
[1]*Department of Mathematics and Physics, Nanjing Institute of Technology, Nanjing 211167, People's Republic of China*
[2]*State Key Laboratory of Surface Physics and Department of Physics, Fudan University, Shanghai 200433, People's Republic of China*
[3]*Department of Physics, The University of Hong Kong, Pokfulam Road, Hong Kong, China*

(Received 19 August 2013; accepted 6 September 2013; published online 23 September 2013)

Within the framework of Hubbard model, a bowtie-shaped graphene nanoflake is identified to undergo an electric-field induced phase transition from an antiferromagnetic ground state. Unlike the case of half-metallic graphene nanoribbons, the electric field here leads to a non-magnetic state instead of ferromagnetic state after destructing the antiferromagnetic ordering. Because the spin is polarized on different sublattices of the nanodot in the antiferromagnetic phase, the transition occurs when the applied field breaks the sublattice symmetry and induces enough energy splitting among the originally degenerate zero-energy states. © *2013 AIP Publishing LLC*. [http://dx.doi.org/10.1063/1.4821954]

Spintronic devices recently attract great interests in potential logic, memory, and communication applications.[1–4] Graphene based nanostructures, because of long spin diffusion length and long lifetime together with high electron velocity, are promising candidates for spintronic applications.[5–9] Recent advances in fabrication technique allow graphene nanoflakes (GNFs) to open up possibilities, for practical applications in nanoelectronic devices.[10–12] For spintronic application, the magnetic properties of GNFs are of vital importance. Compared to armchair-edged GNFs which usually exhibit considerable energy gap and nonmagnetic (NM) ground states,[13–16] the electronic structure and magnetic properties of zigzag-edged GNFs are found highly sensitive to their shapes.[14–20] Zigzag-edged hexagonal and diamond GNFs have antiferromagnetic (AFM) ordering between opposite edges in the ground states,[18–20] while triangular flakes present ferromagnetically (FM) ordered ground states due to the existence of degenerated edge states at $E = 0$ induced by the imbalance between the two sublattices.[14–18]

It has been recently proposed that the magnetic moment of zigzag-edged GNFs can be manipulated by applying an electric field instead of a magnetic field. For example, the total spin of a triangular GNF begin to depolarize when the field strength above a critical value.[21,22] The electric field controlled spin states in GNFs make them suitable to be used as basic components of spintronic devices, such as spin filter and magnetic memory.[23,24] In fact, Son *et al.* first propose that a phase transition from an AFM to FM state can be realized in a graphene nanoribbon with an electric field applied cross its zigzag edges.[25] Later, Zheng and Duley point out that this transition will not happen in rectangular graphene nanodots, instead, the magnetization only found decreasing slowly with the applied field.[26] Recently, Agapito *et al.* show that the transition from an AFM to FM state can be realized in a diamond-shaped graphene nanoflake, however, at a significantly higher electric field.[27]

Similar to rectangular or diamond-shaped GNFs, zigzag bowtie-shaped GNFs (zBGNFs) have balanced sublattices and AFM ground states.[28,29] However, these zBGNFs also have zero-energy states like those triangular GNFs. The existence of zero-energy states makes the electronic structure and then magnetic ordering of the system vulnerable by an applied electric field, which suggests that a zBGNF be a perfect candidate to realize AFM-NM phase transition at a reasonably low electric field. In this letter, we will study the effect of an applied electric field on the edgestate magnetism in zBGNFs to explore an efficient electrical control of magnetic ordering in nanographene structures.

Within the mean-field approximation of Hubbard model, the Hamiltonian of a zBGNF is given by

$$H = \varepsilon \sum_{i\sigma} c_{i\sigma}^{+} c_{i\sigma} + t \sum_{\langle ij \rangle \sigma} (c_{i\sigma}^{+} c_{j\sigma} + h.c.) + U \sum_{i\sigma} n_{i\sigma} \langle n_{i,-\sigma} \rangle, \quad (1)$$

where $\varepsilon = 0$ is the on-site energy, $t = -2.7\,\text{eV}$ is the hopping energy between the nearest-neighbor atoms, $c_i^{+}(c_i)$ is the creation (annihilate) operator of π electron with spin σ at site i, $U = t$ is the on-site Coulomb repulsion, and $n_{i\sigma} = c_{i\sigma}^{+} c_{i\sigma}$ is the spin-resolved density at site i.

Figure 1 shows a zBGNF with $N = 5$ and $m = 2$ as our model system, where N and m is the number of benzene rings on each triangular side and junction, respectively. A transverse electric field is applied within the plane from the left side to the right. In the absence of electric field, the degeneracy of zero-energy states in zBGNFs is determined by $2(N - m - 1)$. Here, two of the four zero-energy states are localized on one sublattice in the left triangular part while the other two states only arise on the other sublattice in the right part. However, the overall sublattice polarization is zero.

Figure 2 plots the energy levels of the zBGNF as a function of the applied transverse electric field. The most noticeable is that degeneracy of the zero-energy states is lifted and the energy separation increases almost linearly with the field. As a result, the single-particle energy gap between the highest occupied molecular orbital (HOMO) and the lowest unoccupied molecular orbital (LUMO) can be described by the linear Stark effect, i.e., $E_g/t \approx 3.77\,\text{F}$. The originally degenerate zero-energy states are seen to form two pairs of

a)Email: shengw@fudan.edu.cn

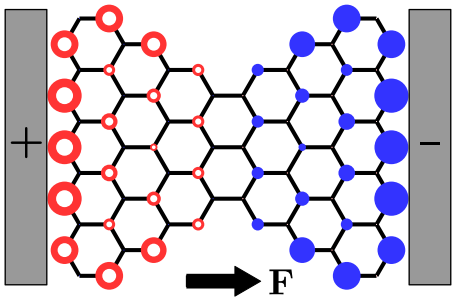

FIG. 1. A schematic view of a zBGNF with $N = 5$ and $m = 2$ sandwiched by two electrodes. Solid and open dots denote the overall electron densities of the degenerate zero-energy states located at two different sublattices.

states, one above the zero line and the other one below. The energy splitting within these pairs, ΔE as indicated by the arrows, is about one-fifth of E_g. In spite of the energy separations induced by the electric field, the original zero-energy edge states keep strongly localized. In the meantime, the overall sublattice polarization for these states remains zero.

In the absence of electric field, it has been shown that the zBGNF has an AFM ground state due to the spatially separated edge states of high energy degeneracy. The spin density of the ground state obtained by solving the mean-field Hubbard Hamiltonian self-consistently looks very similar to that as shown in Fig. 1. Since the total spin of an AFM ordering is always zero, here we make use of the largest local magnetic moment of carbon atoms in the ground state, M_{max}, to describe the spin polarization. At zero field, we find that $M_{max} \approx 0.295\,\mu_B$. Figure 3 plots the maximum magnetization as a function of the applied electric field. It is seen that M_{max} remains almost constant for the applied field up to $F_c = 0.0396$ V/Å. After this critical field, M_{max} is seen to jump directly to zero and the whole magnetization vanishes, which reflects the destruction of the AFM ordering and a clear phase transition from AFM to NM.

The dramatic transition from an AFM to NM ordering in the ground state of the zBGNF can be attributed to the competition between the Coulomb interactions and the kinetic energy induced by the applied electric field. The former is represented by the energy separation between the AFM ground state and FM first excited state, i.e., $2J = E_{FM} - E_{AFM}$, which

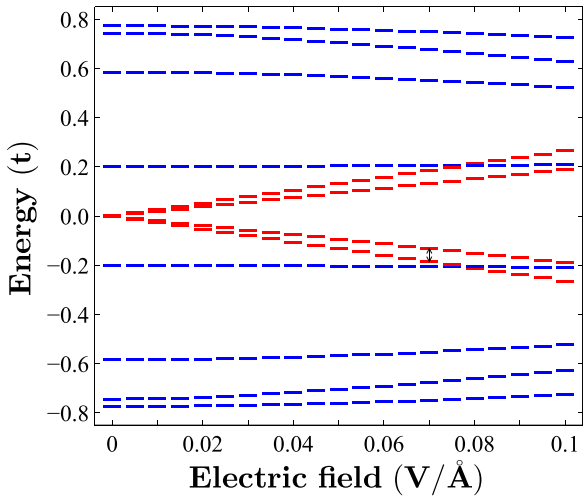

FIG. 2. Energy spectrum of the zBGNF in the presence of the applied transverse electric field. The energy splitting ΔE is indicated by the arrows.

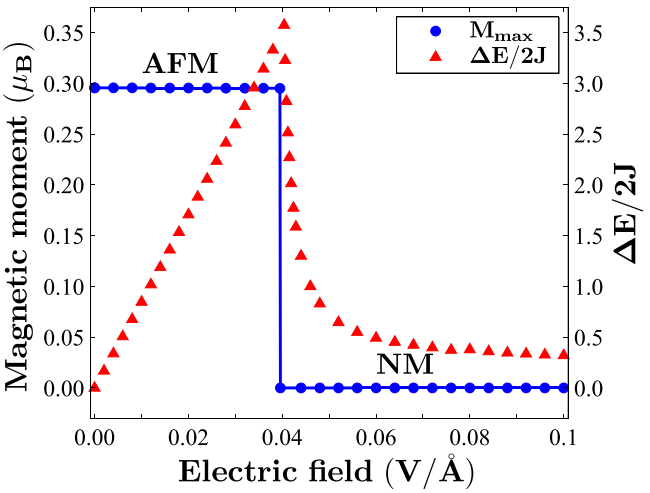

FIG. 3. The largest local magnetic moment and the ratio between the single-particle energy splitting and AFM coupling calculated as a function of the applied electric field.

is also known as the AFM coupling. In the NM phase, the ground state becomes non-magnetic and correspondingly $2J = E_{FM} - E_{NM}$. The latter is denoted by the single-particle energy splitting ΔE induced by the applied field. Figure 3 plots the ratio $\Delta E/2J$ as a function of the applied field. The ratio starts with zero thanks to the degenerate zero-energy states at zero field. In the AFM phase, we find that the coupling keeps almost a constant value of 24.2 meV and hence the ratio increases in proportion with the field. As the applied field increases close to F_c, the energy splitting between the two topmost occupied states becomes large enough to override the AFM coupling, which results in the phase transition to the NM state. After the transition, the energy gap $E_{FM} - E_{NM}$ becomes increasing linearly with the field, and therefore the ratio is found to drop rapidly within a very small field range and then slowly decays.

Beyond the mean-field approximation, we make use of a configuration-interaction (CI) approach to study the magnetic phase transition induced by the applied electric field. A full CI with a total of 28 single-particle states, which generates tens of millions Slater determinants,[30] gives a similar critical field around 0.04 V/Å. Like the result by the mean-field approximation, the AFM coupling is noted to first decrease before the transition and then the gap increases dramatically after the transition.

Next, let us have a closer look at the spin configuration before and after the transition. The mean-field approximation of the Hubbard model is solved by using the unrestricted scheme, i.e., allowing spin up and spin down states to evolve separately. Figure 4 plots the energy levels obtained by a self-consistent calculation at zero field, one before and one after the transition. At zero field it is noticed that, even within the unrestricted scheme, spin-up and spin-down states share the same energy spectrum with the electron-hole symmetry,

$$E_{i,\uparrow} = E_{i,\downarrow} = E_{N_t-i,\uparrow} = E_{N_t-i,\downarrow},$$
$$|\varphi_{i,\uparrow}|^2 = |\varphi_{N_t-i,\downarrow}|^2, \tag{2}$$

with N_t being the total number of electrons. It is further seen that the Coulomb interaction lifts the degeneracy of the four

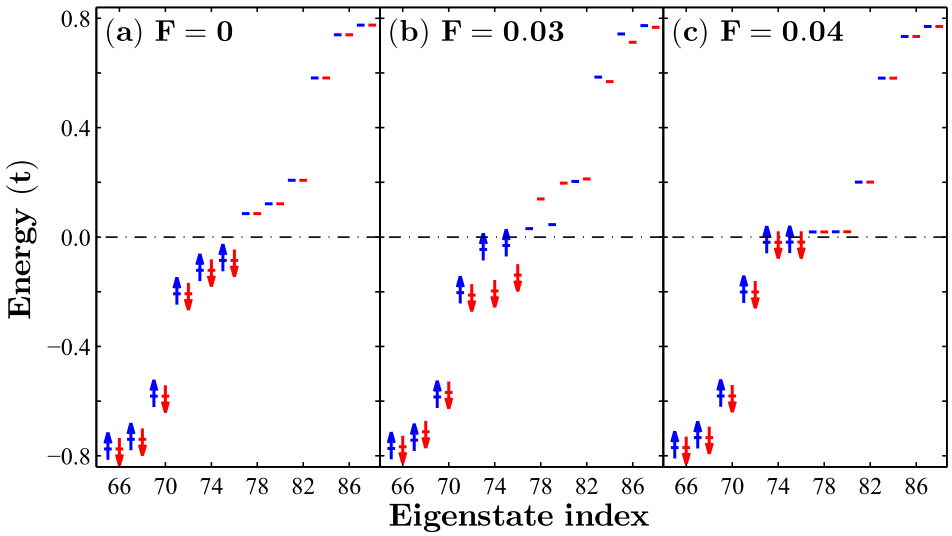

FIG. 4. Energy levels of the zBGNF obtained by solving a mean-field Hubbard model self-consistently at three different electric fields, (a) $F = 0$, (b) $F = 0.03$ V/Å, and (c) $F = 0.04$ V/Å.

zero-energy states and splits them into two degenerate pairs of states. Here, spin degeneracy remains intact and each energy level is doubly occupied. The total spin of the system is therefore zero. Nevertheless, the spin-up and spin-down states at the same energy level have different electron densities, i.e., $|\varphi_{i,\uparrow}|^2 \neq |\varphi_{i,\downarrow}|^2$. Hence the spin is locally polarized even when the overall spin is zero. In the zBGNF, spin degeneracy and sublattice symmetry are correlated. When the latter is broken by the applied electric field, the former can no longer exist. Figure 4(b) shows that the spin degeneracy is lifted at $F = 0.03$ V/Å just before the critical field. Now, the spin-up and spin-down states have not only different density distributions but also splitting energy levels. In the meantime, the electron-hole symmetry is also broken, i.e., $E_{i,\uparrow} \neq E_{N_t-i,\uparrow}$. As a result, the up-spin gap decreases while the down-spin gap increases greatly.[25]

Figure 5(a) plots the corresponding spin density of the ground state. Although the energy spectrum changes dramatically with the field, the spin density at $F = 0.03$ V/Å is seen to have a very similar distribution to that at zero field. As the electric field further increases to 0.04 V/Å beyond the threshold value 0.0396 V/Å, it can be seen from Fig. 4(c) that the spin degeneracy recovers and the energy spectrum becomes similar to that at the zero field except for much smaller energy gap around the Fermi level. The other important difference is that the electron densities of the degenerate spin-up and spin-down states are now identical. As a result, the local spin polarization totally vanishes across the whole structure and the ground state becomes NM, as shown in Fig. 5(b).

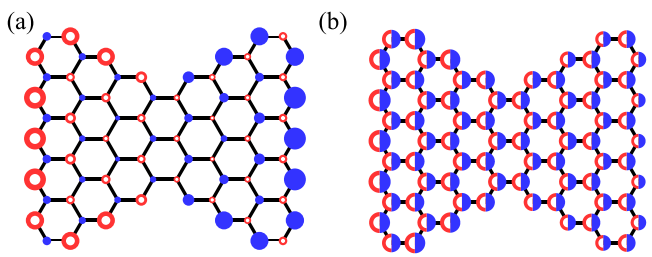

FIG. 5. Ground state spin density in the zBGNF at (a) $F = 0.03$ V/Å and (b) $F = 0.04$ V/Å. Solid and open dots denote two different spin components.

We have seen that the electric field induces local spin transfer between the two triangles of the zBGNF by breaking the sublattice symmetry and finally leads to the destruction of the AFM ordering without resort to spin-orbit coupling. Although the applied electric field first closes the energy gap for one spin orientation while widening the other in the zBGNF similar to graphene nanoribbons[25] or diamond-shaped graphene nanoflakes,[27] a different phase transition which results in a NM state instead of a FM state occurs when the field exceeds the threshold. Without the help of degenerate zero-energy states, the transition from an AFM to NM state in rectangular GNFs is shown to require a much stronger electric field.[26] Moreover, the transition in the rectangular nanodot occurs slowly over a large field range (>0.1 V/Å). In contrast, the electrical switching of the AFM state in the zBGNF occurs almost instantly after the critical field.

Finally, we present the ground state phase diagram of the zBGNF calculated for the range $1.0 \leq U/t \leq 2.0$ in Fig. 6. It is seen that the critical field for the transition to the nonmagnetic state increases almost quadratically with the Hubbard U. At $U/t = 2.0$, the field reaches 0.114 V/Å. This is understood by the fact that the AFM coupling in the Hubbard model becomes stronger as the Hubbard U increases, and

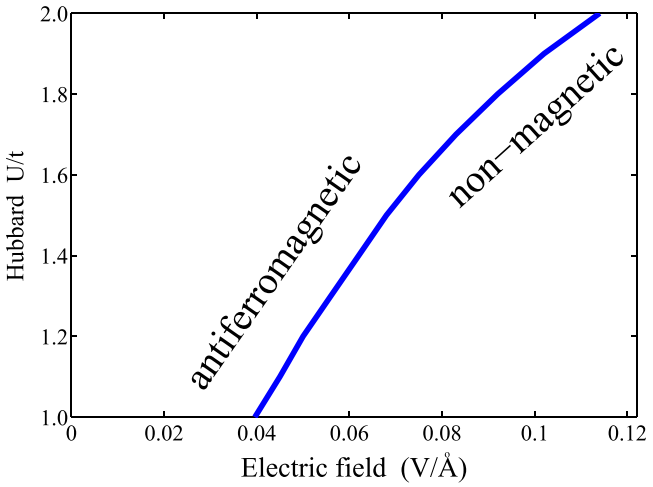

FIG. 6. Ground state phase diagram of the zBGNF for $1.0 \leq U/t \leq 2.0$.

therefore requires higher electric field for destructing the antiferromagnetic ordering.

In summary, we have studied electrical control of spin configuration in bowtie-shaped graphene nanodots. Within the framework of mean-field Hubbard model, we have demonstrated that the antiferromagnetic ordering in the ground state of the nanodot can be efficiently switched by applying an electric field. The local maximum magnetic moment of the antiferromagnetic ground state is shown to be almost constant for the field up to 0.04 V/Å while vanishes abruptly as the applied field exceeds the critical field. Unlike half-metallic graphene nanoribbons, we have revealed that the electric field induces a phase transition to non-magnetic state instead of ferromagnetic state after the destruction of antiferromagnetic ordering. Finally, we have obtained the ground state phase diagram for the graphene nanoflake.

This work was supported by National Basic Research Program of China (973 Program No. 2011CB925602). Xu would like to acknowledge the support by Shenzhen Basic Research Grants (No. JCYJ20120615142933076).

[1]S. A. Wolf, D. D. Awschalom, R. A. Buhrman, J. M. Daughton, S. von Molnàr, M. L. Roukes, A. Y. Chtchelkanova, and D. M. Treger, Science **294**, 1488 (2001).
[2]A. Ney, C. Pampuch, R. Koch, and K. H. Ploog, Nature **425**, 485 (2003).
[3]H. Dery, P. Dalal, L. Cywiński, and L. J. Sham, Nature **447**, 573 (2007).
[4]B. Behin-Aein, D. Datta, S. Salahuddin, and S. Datta, Nat. Nanotechnol. **5**, 266 (2010).
[5]N. Tombros, C. Jozsa, M. Popinciuc, H. T. Jonkman, and B. J. van Wees, Nature **448**, 571 (2007).
[6]O. V. Yazyev and M. I. Katsnelson, Phys. Rev. Lett. **100**, 047209 (2008).
[7]W. Han, K. Pi, W. Bao, K. M. McCreary, Y. Li, W. H. Wang, C. N. Lau, and R. K. Kawakamib, Appl. Phys. Lett. **94**, 222109 (2009).
[8]T.-Y. Yang, J. Balakrishnan, F. Volmer, A. Avsar, M. Jaiswal, J. Samm, S. R. Ali, A. Pachoud, M. Zeng, M. Popinciuc, G. Gütherodt, B. Beschoten, and B. Özyilmaz, Phys. Rev. Lett. **107**, 047206 (2011).
[9]T. Maassen, J. J. van den Berg, E. H. Huisman, H. Dijkstra, F. Fromm, T. Seyller, and B. J. van Wees, Phys. Rev. Lett. **110**, 067209 (2013).
[10]K. A. Ritter and J. W. Lyding, Nature Mater. **8**, 235 (2009).
[11]L. C. Campos, V. R. Manfrinato, J. D. Sanchez-Yamagishi, J. Kong, and P. Jarillo-Herrero, Nano Lett. **9**, 2600 (2009).
[12]G. M. Rutter, N. P. Guisinger, J. N. Crain, P. N. First, and J. A. Stroscio, Phys. Rev. B **81**, 245408 (2010).
[13]Z. Z. Zhang, K. Chang, and F. M. Peeters, Phys. Rev. B **77**, 235411 (2008).
[14]H. P. Heiskanen, M. Manninen, and J. Akola, New J. Phys. **10**, 103015 (2008).
[15]M. Zarenia, A. Chaves, G. A. Farias, and F. M. Peeters, Phys. Rev. B **84**, 245403 (2011).
[16]J. Akola, H. P. Heiskanen, and M. Manninen, Phys. Rev. B **77**, 193410 (2008).
[17]M. Ezawa, Phys. Rev. B **76**, 245415 (2007).
[18]J. Fernández-Rossier and J. J. Palacios, Phys. Rev. Lett. **99**, 177204 (2007).
[19]S. Bhowmick and V. B. Shenoy, J. Chem. Phys. **128**, 244717 (2008).
[20]H. Feldner, Z. Y. Meng, A. Honecker, D. Cabra, S. Wessel, and F. F. Assaad, Phys. Rev. B **81**, 115416 (2010).
[21]P. Potasz, A. D. Cüçlü, A. Wójs, and P. Hawrylak, Phys. Rev. B **85**, 075431 (2012).
[22]W. L. Ma and S. S. Li, Phys. Rev. B **86**, 045449 (2012).
[23]B. Trauzettel, D. V. Bulaev, D. Loss, and G. Burkard, Nat. Phys. **3**, 192 (2007).
[24]M. Ezawa, Eur. Phys. J. B **67**, 543 (2009).
[25]Y.-W. Son, M. L. Cohen, and S. G. Louie, Nature **444**, 347–349 (2006).
[26]H. X. Zheng and W. Duley, Phys. Rev. B **78**, 155118 (2008).
[27]L. A. Agapito, N. Kioussis, and E. Kaxiras, Phys. Rev. B **82**, 201411(R) (2010).
[28]W. L. Wang, O. V. Yazyev, S. Meng, and E. Kaxiras, Phys. Rev. Lett. **102**, 157201 (2009).
[29]M. Kinza, J. Ortloff, and C. Honerkamp, Phys. Rev. B **82**, 155430 (2010).
[30]W. Sheng, M. Sun, and A. Zhou, Phys. Rev. B **88**, 085432 (2013).